

1 **Sylites: Multipurpose markers for the** 2 **visualization of inhibitory synapses**

3 **Vladimir Khayenko¹, Clemens Schulte^{1†}, Sara L. Reis^{2†}, Orly Avraham³, Cataldo Schietroma⁴, Rafael**
4 **Worschech¹, Noah F. Nordblom¹, Sonja Kachler¹, Carmen Villmann², Katrin G. Heinze¹, Andreas**
5 **Schlosser¹, Ora Schueler-Furman³, Philip Tovote^{2,6}, Christian G. Specht^{5*}, Hans Michael Maric^{1*}**

6 [†]These authors contributed equally to the manuscript

7 *Correspondence to christian.specht@inserm.fr, hans.maric@uni-wuerzburg.de

8 ¹Rudolf Virchow Center; Center for Integrative and Translational Bioimaging; University of Wuerzburg; Josef-
9 Schneider-Str. 2, 97080 Wuerzburg, Germany

10 ²Institute of Clinical Neurobiology, University Hospital, Versbacher Str. 5, 97078 Wuerzburg, Germany

11 ³Department of Microbiology and Molecular Genetics, Institute for Medical Research Israel-Canada, the
12 Hebrew University, Hadassah Medical School, Jerusalem 91120, Israel

13 ⁴Abbelight, 191 Avenue Aristide Briand, 94230 Cachan, France

14 ⁵Diseases and Hormones of the Nervous System (DHNS), Inserm U1195, Université Paris-Saclay, 80 rue du
15 Général Leclerc, 94276 Le Kremlin-Bicêtre, France

16 ⁶Center of Mental Health, University of Wuerzburg, Margarete-Höppel-Platz 1, 97080 Wuerzburg, Germany

17 **Abstract**

18 **We introduce Sylites – small and versatile fluorogenic affinity probes for high-contrast**
19 **visualization of inhibitory synapses. Having stoichiometric labeling and exceptional selectivity for**
20 **neuronal gephyrin, a hallmark protein of the inhibitory post-synapse, Sylites enable superior**
21 **synapse staining compared with antibodies. Combined with super-resolution microscopy, Sylites**
22 **allow precise nanoscopic measurements of the synapse. In brain tissue, Sylites reveal the three-**
23 **dimensional distribution of inhibitory synapses within just an hour.**

24 **Main**

25 Reliable markers that visualize synapses, and, by extension, neural circuits, have great value for
26 clinical and fundamental neuroscience¹. An integral component of inhibitory synapses is gephyrin, a
27 highly abundant scaffold protein that stabilizes glycine and GABA_A receptors^{2,3}. Gephyrin serves as a
28 universal marker of the inhibitory synapse and its concentration at the post synaptic density closely
29 correlates with the number of inhibitory receptors and the synaptic strength⁴⁻⁶. Gephyrin is commonly
30 visualized using antibodies⁷ or recombinant techniques that tag gephyrin with fluorescent proteins⁸,
31 but these approaches come with caveats: recombinant proteins are prone to overexpression, their use
32 in complex organisms is challenging and they cannot be applied if wild-type species are to be studied.
33 Antibodies, on the other hand, do not require genetic manipulation and are easily applicable in fixed
34 samples; however, their large size and the tendency to crosslink affect the labeling performance in
35 complex samples⁹. Here we introduce selective high affinity stoichiometric probes for gephyrin that
36 enable high-contrast visualization of synapses in cell cultures and tissue and deliver accurate super-
37 resolution measurements.

38 The first probe that exploited a definite feature of synaptic gephyrin, a universal receptor binding
39 pocket in the gephyrin E domain, was TMR2i¹⁰. This probe was derived from the intracellular loop of
40 the glycine receptor (GlyR) β subunit, a natural ligand of this docking site, as are multiple members of
41 the synaptic GABA_AR subtypes^{11,12}. TMR2i did bind gephyrin but gave low-contrast labeling and was
42 not suitable for nanoscopy, such as direct stochastic optical reconstruction microscopy (dSTORM).

43 We systematically optimized both the probe architecture and the gephyrin binding sequence to target
44 the native protein (Fig.S1, Tables S2,4,5), and synthesized an array of fluorescent probes. We then
45 performed an imaging-based evaluation of the probes for the binding of gephyrin in fixed cells
46 (Fig.S2, Fig.S3). SyliteM, a monomeric probe with strictly linear gephyrin labeling (Fig.S2), and
47 SyliteD, a dimeric probe (Fig.1a) with higher affinity and contrast, displayed the highest target to off-
48 target labeling ratios and a strong linear relationship with gephyrin (Fig.S2).

49 Sylites showed a near-complete correlation with gephyrin in COS-7 cells expressing recombinant
50 eGFP-gephyrin, and no correlation with cells expressing soluble eGFP. Notably, the target to off-
51 target labeling ratios of SyliteM and SyliteD were ~35 and ~500, respectively, approximately 10 and
52 150-fold higher than those of TMR2i (Fig.1b,c, Fig.S3). Using isothermal titration calorimetry (ITC)
53 with gephyrin E domain, we determined a K_d of 17.5 ± 2.8 nM for the dimeric SyliteD and a K_d of
54 205 ± 102 nM for the monomeric SyliteM, indicating high probe affinity, and confirming the
55 stoichiometric binding of 1:1 for SyliteM and 1:2 for SyliteD (Fig.1d), in line with their monomeric
56 and dimeric design. Lastly, mass-spectrometric determination of the interactomes of Sylites confirmed
57 their target selectivity. Gephyrin was the only protein with high abundance, high selectivity and
58 multiple unique peptide fragments binding to the dimeric probe. The monovalent probe retained some
59 additional proteins other than gephyrin, consistent with its somewhat lower target to off-target
60 labeling ratio.

61 Gephyrin is a multifunctional protein with numerous isoforms and post-translational modifications¹³.
62 Comparison of the binding profiles to eleven major gephyrin isoforms expressed in HEK293 cells
63 (Fig.1f, Fig.S4) reveals that Sylites, but not the tested antibodies, exclusively label gephyrin isoforms
64 that have GlyR and GABA_A receptor binding capacity. This indicates that Sylites are ideally suited to
65 detect synapses and to quantify functionally relevant receptor binding sites. Interestingly, no gephyrin
66 labeling was observed with the widely used mAb7a antibody in HEK293 cells. Microarray profiling
67 of mAb7a binding (Fig.S5) confirms that in contrast to Sylites, mAb7a depends on a phosphorylated
68 (pSer270) epitope in the linker region of gephyrin¹⁴. Thus, mAb7a labels only a sub-population of
69 synaptic gephyrin isoforms and phosphorylation variants.

70 We next used the probes to study the structure and distribution of inhibitory synapses in brain sections
71 and cultured neurons using conventional and super-resolution microscopy. In cortical neurons
72 expressing gephyrin-mEos2 fluorescent protein chimera, we observed high contrast visualization of
73 densely packed gephyrin clusters at synapses and a near complete correlation of Sylite staining with
74 gephyrin (Fig.2a,b). Target specificity was confirmed by Sylite overlap with endogenous antibody-
75 labeled gephyrin in wild-type cortical and hippocampal neurons (Fig.S6). Linear regression analysis
76 of fluorescent intensities of synaptic mEos2-gephyrin puncta with correspondent Sylite or mAb7a-
77 stained puncta revealed a 3- and 2-time narrower prediction interval for SyliteM and SyliteD,
78 respectively, compared with mAb7a, indicating a much closer relation between Sylite and mEos2-
79 gephyrin signals (Fig.2c). The higher scattering observed with mAb7a, suggests that the antibody
80 staining exhibits non-linear scaling with synaptic gephyrin, in agreement with our previous findings
81 on the selectivity of mAb7a for a specific, phosphorylated variant of gephyrin (Fig.S5). Taken
82 together, our data demonstrate a linear, stoichiometric relationship between Sylites and gephyrin,
83 making them suitable for quantitative microscopy¹⁵.

84 Consequently, we conducted super-resolution nanoscopic distance measurements between the
85 neuronal pre- and post-synapse using our probe and gephyrin antibodies. We carried out dSTORM
86 experiments, focusing on the dimeric SyliteD due to its suitable blinking properties. Cortical neurons
87 were labeled for gephyrin and RIM, a protein of the presynaptic active zone (AZ), using SyliteD

88 together with primary anti-RIM1/2 and CF680-conjugated secondary antibodies (Fig.2d,e). Dual-
89 color 3D-dSTORM images show that the SyliteD detections closely match the distribution of RIM in
90 the AZ, confirming a recent finding of a strong association between RIM and gephyrin sub-synaptic
91 domains⁴. The measured Euclidian distance between SyliteD and RIM1/2-CF680 was 129 ± 24 nm
92 (mean \pm SD), in agreement with the estimated molecular sizes separating the two labels¹⁶. The direct
93 comparison with mAb7a and mAb3B11 labeling confirmed that SyliteD provides a precise read-out
94 for the location of synaptic gephyrin and receptor binding sites at inhibitory synapses (Fig.2f).

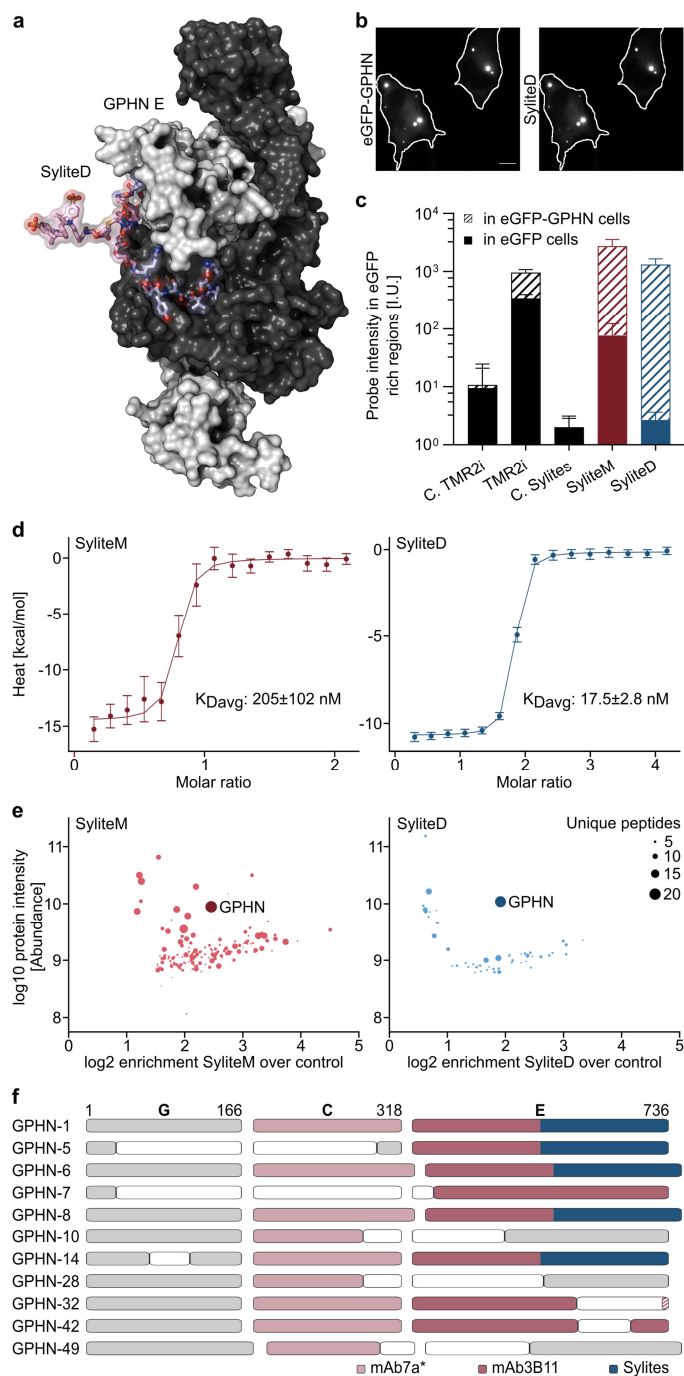
95 Determining the organization, distribution and integrity of inhibitory synapses in brain tissue is of
96 central importance for a wide range of neurobiological topics, from neural circuits to neuropathology.
97 Until now, tissue staining of inhibitory synapses has been an elaborate and time-consuming procedure
98 that was generally limited to relatively thin brain sections (≤ 16 μ m) to obtain reliable labeling⁷. Here
99 we demonstrate that Sylites, owing to their small size, effectively penetrate 50 μ m-thick tissue
100 sections, achieving high-contrast labeling within one hour, using a standard, immunohistochemistry
101 protocol. We visualized inhibitory synapses and their distribution using epifluorescence microscopy
102 with 20X magnification, giving us a macro-overview of the inhibitory synapse distribution in brain.
103 (Fig.2g). Next, we incubated brain hippocampal sections for 1, 24 and 72 hours with Sylites and with
104 mAb3B11 or mAb7a, then imaged the sections with a confocal microscope, deconvoluted the image
105 stacks, and reconstructed 3D images. Sylite-visualized synapses were observed in the *stratum oriens*
106 of the CA3 region of the ventral hippocampus, an area packed with inhibitory interneurons¹⁷
107 (Fig.2g,h, MovieS1). Sylites detected synaptic clusters throughout the entire section, demonstrating a
108 complete penetration of the probe, already after 1 hour of incubation (MovieS2,3), and even after 72
109 hours of incubation with Sylites, we did not observe any significant background fluorescence
110 (MovieS4,5). In contrast, after 24 hours, the antibody labeling was strongest near the surface of the
111 section while the center remained largely unlabeled (Fig.2i-j, MovieS1,6). Antibody penetration
112 improved after 72 hours; however, background staining was also higher (Fig.S7, MovieS4,5). This is
113 seen by the drop in the overlap between antibody and Sylite labeling from ~ 0.4 for both 7a and 3B11
114 antibodies after 24h to ~ 0.1 after 72 hours (Fig.S7b). Lastly, 3D visualization of synapses produced
115 by Sylites showed smooth, elongated and well-defined shapes of different sizes, in agreement with the
116 known diversity of inhibitory synapses in the CNS¹⁸. After 24 hours, the antibodies produced both
117 smooth and amorphous clusters, and after 72 hours, this pattern changed to primarily amorphous
118 clusters and loss of any observable cluster directionality (MovieS7,8).

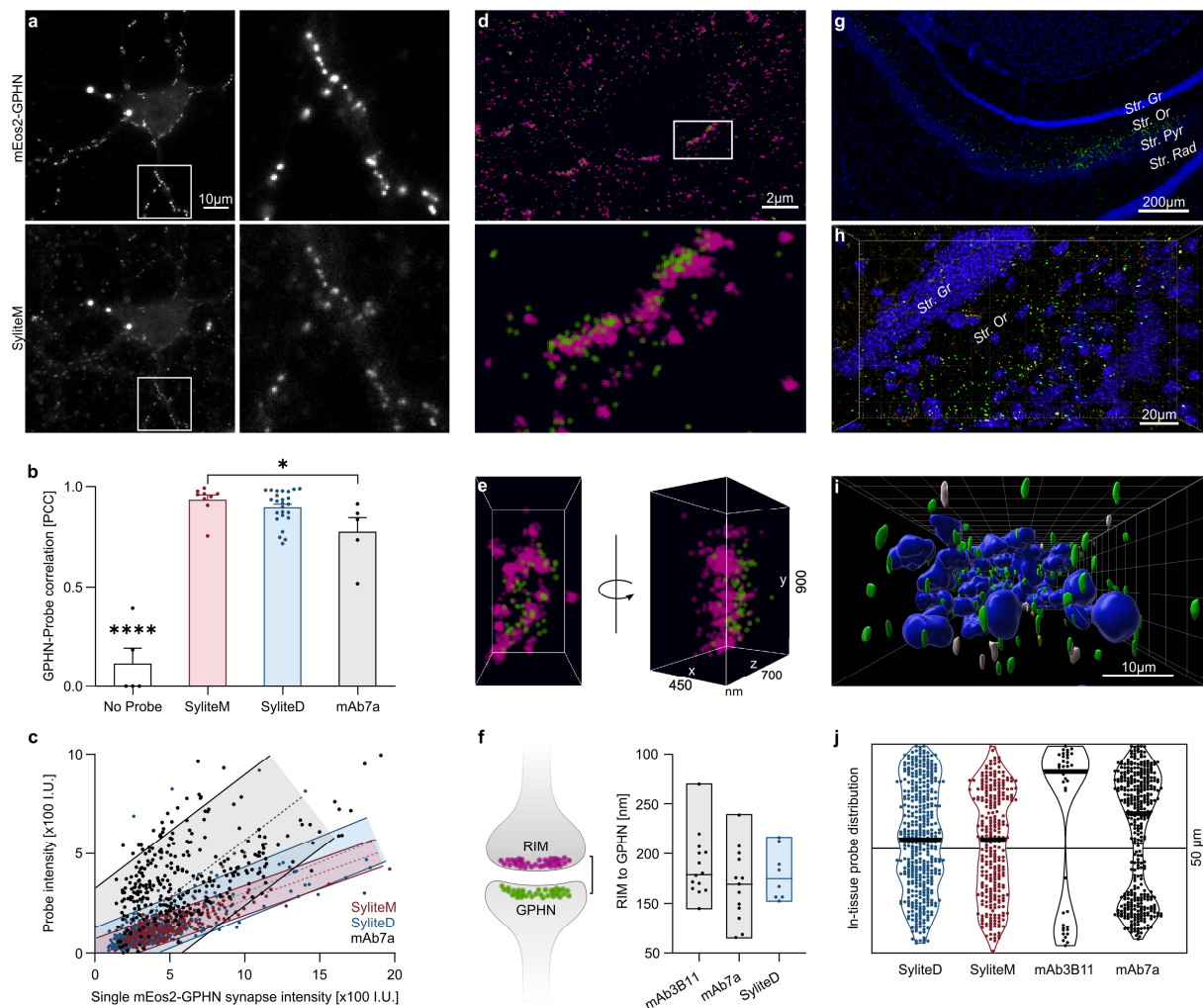
119 The past decades have seen a surge in technological advances in fluorescent microscopy and labeling
120 methods, creating a demand for new probes, particularly for neurosciences, where micro- and
121 nanoscale studies are required to decipher brain function¹. However, only a handful of small affinity
122 probes are available for fluorescence microscopy to date; the most prominent example is the widely
123 used and easily applied DNA label DAPI. Sylites possess the same essential qualities as DAPI,
124 namely high contrast visualization together with fast and reproducible staining protocols. Sylites bind
125 neurotransmission-relevant gephyrin isoforms, acting as universal labels of inhibitory synapses, and
126 their labeling linearity and defined stoichiometry enable deep quantification of the synapses. Our
127 findings demonstrate that small affinity probes can be used adjuvant to antibodies or as their
128 substitution, as they can be smartly designed to bind specific targets, and their small size effectively
129 enables faster distribution, better penetration and staining in biological samples.

130 To summarize, our findings establish Sylites as powerful, versatile and reliable bioimaging tools for
131 neuroscience. We anticipate that next-generation affinity probe development will continue to gather
132 pace, as their synergy with cutting-edge microscopy is indisputable and will help to decipher brain
133 cell organization and function.

134 **Figure 1. Sylites selectively and stoichiometrically**
 135 **bind gephyrin, enabling high contrast imaging.**

136 **a.** Rosetta FlexPepDock structural model of SyliteD
 137 bound to gephyrin (GPHN) E domain dimer. In blue
 138 is the binding sequence, in pink is the linker and the
 139 fluorophore, the two gephyrin E domains in black
 140 or white. **b.** Left: Fixed COS-7 cells expressing eGFP-
 141 gephyrin, Right: SyliteD 50 nM staining of the fixed
 142 sample. Scale bar 10 μ m. **c.** Labeling contrast of the
 143 peptide-based probes. The Y axis represents log
 144 average signal intensity of the probe signal from
 145 eGFP-rich regions of the COS-7 cells. SyliteM and
 146 SyliteD have \sim 35 and \sim 500 target to off-target
 147 labeling ratio, respectively, TMR2i has a target to
 148 off-target labeling ratio of \sim 3. C.TMR2i represents
 149 red spectrum readouts of unlabeled cells. C.Sylites
 150 represents far-red spectrum readouts of unlabeled
 151 cells. $n \geq 8$. Mean \pm SD. **d.** ITC measured heat
 152 signature of SyliteM and SyliteD titrated with
 153 gephyrin E domain. Both probes exhibit nanomolar
 154 affinity, with SyliteD having 10-fold affinity increase
 155 over the monomer. **e.** Sylites selectively pull
 156 gephyrin. Quantitative mass spectrometric analysis
 157 of SyliteM/D pull-downs. Non-fluorescent versions
 158 of SyliteM and SyliteD were used to pull down
 159 proteins from mouse brain homogenate and the
 160 protein fractions were subsequently digested and
 161 analyzed with LC-MS/MS. The size of the circle
 162 corresponds to the number of unique peptides
 163 identified for the specific protein. Left: SyliteM
 164 pulls down additional proteins that have high
 165 intensity and are abundant in its pool, although
 166 gephyrin is the most prominent. Right: gephyrin
 167 is a single protein with high abundance, selectivity
 168 and strong representation in the SyliteD pull-down.
 169 **f.** Sylites bind synaptic gephyrin. Probe interaction
 170 with gephyrin isoforms. The isoform GPHN-1
 171 represents the primary structure of gephyrin¹⁹. The
 172 protein consists of 3 regions: G domain, C unstructured
 173 linker region, E domain, where the receptor-binding
 174 pocket is located. Blank boxes indicate deletions,
 175 elongated boxes – additions, striped boxes –
 176 substitutions. The peptide probes (blue) bind to
 177 isoforms that can form a receptor binding pocket
 178 of the E domain. The antibodies bind both
 competent and incompetent receptor clustering
 isoforms. mAb7a (rose) binds a short linear
 *Ser270 phosphorylated epitope in the “C” linker
 region, while mAb3B11 (raspberry) interacts with
 an epitope in the E domain.





179
180
181
182
183
184
185
186
187
188
189
190
191
192
193
194
195
196
197
198
199
200
201
202
203
204

Figure 2. Sylites: versatile probes to visualize inhibitory synapses. a-d. Sylites enable linear visualization of inhibitory synapses in neuronal cultures. a. Top: Fixed cortical neurons expressing mEos2-gephyrin, bottom: SyliteM 50 nM staining of the fixed sample. Right: zoom in on the boxed region. SyliteM stains recombinant and endogenous gephyrin. **b.** Pearson's correlation coefficients (PCC) of mEos2-gephyrin expressing neurons with the counterstain of SyliteM, SyliteD or mAb7a. All probes show high correlation to the recombinant neurons. Mean±SEM. Significance determined using one-way ANOVA with a follow up Tukey's test for multiple comparisons. * P<0.05, **** P<0.0001. **c.** Intensity dependence of single mAb7a or Sylite labeled synapses to the reference mEos2-gephyrin synapse signal intensity. Much higher signal scattering is observed with mAb7a (grey), while both SyliteM (red) and SyliteD (blue) have a constant linear labeling behavior. Shaded regions indicate a 90% prediction interval. 10 pairs of images were used for each probe. **d-f. Super-resolution imaging and nanometric measurements with SyliteD. d.** Top: dSTORM of neuronal synapses with presynaptic RIM labeling with RIM1/2-CF680 antibody (magenta) and postsynaptic gephyrin labeling with SyliteD (green). Bottom: zoomed region. **e.** Side and *en face* view of a single synapse **f.** Nanometric distance measurement with SyliteD. RIM to gephyrin center of mass distance measurements conducted with RIM1/2-CF680 and either gephyrin antibodies or SyliteD. In all cases an average distance of ~130 nm was calculated. Bars indicate the full range of individual measurements, the in-bar line indicates the median. **g-j. Sylites reveal the distribution of inhibitory synapses in hippocampal sections. g.** Wide field 2D image of ventral hippocampus section stained with DAPI (blue) and SyliteD (green). Gephyrin staining is visible in the *stratum oriens* of the CA3 region of the ventral hippocampus. Str. Rad – Stratum Radiatum; Str. Pyr – Stratum Pyramidal; Str. Or – Stratum Oriens; Str. Gr – Stratum Granulosum. **h.** Confocal microscopy. 3D top view of SyliteD and mAb3B11 24-hour co-staining of ventral hippocampus section. Green – SyliteD, gold – mAb3B11, blue – DAPI nuclear staining. Numerous synapses are visible with SyliteD staining, mAb3B11 produces fewer detections. Synapses appear in the *stratum oriens*. **i.** 3D volumetric representation of nuclei and inhibitory synapses. Side view of a section co-labeled for gephyrin for 24 hours with SyliteD and mAb3B11. Green – SyliteD, gold – mAb3B11, blue – DAPI nuclear staining. In white SyliteD and mAb3B11 co-labeled synapses. **j.** Distribution of detected synapses in 50 μm-thick hippocampal sections after 24-hour staining. Violin plot represents the labeled synapse distribution. Thick black lines - median Z position of detected synapses. The hourglass shape of antibody labeling indicates skewed antibody distribution, towards the surfaces of sections.

205 Acknowledgements

206 We thank Dr. Jens Vanselow, Stephanie Lamer and Alvaro Ciudad for supporting the mass spectrometric studies and
207 analysis. We thank Prof. Eric Allemand and Dr. Fabrice Ango for providing gephyrin isoform constructs. And we
208 thank Dr. Katharina Hemmen, Dr. Hanna Heil, Mike Friedrich and Jürgen Pinnecker for their guidance in 3D image
209 analysis and light microscopy.

210 Funding

211 H.M.M. acknowledges financial support from the Deutsche Forschungsgemeinschaft (DFG MA6957/1-1 and TRR
212 166 ReceptorLight, project B05).

213 Author Contributions

214 Conceptualization, H.M.M, V.K., Methodology, H.M.M, C.G.S., V.K., C.S., S.L.R., O.A., C.V., K.H. A.S., O.S.F.,
215 P.T., Formal Analysis, H.M.M, C.G.S., V.K., C.S., S.L.R., O.A., A.S., O.S.F., P.T.; Investigation, H.M.M, C.G.S.,
216 V.K., C.S., S.L.R., O.S.F., R.W., N.F.N, S.K., C.V.; Writing – Original Draft Preparation, H.M.M. and V.K.; Writing
217 – Review & Editing, H.M.M., V.K., C.G.S., C.S. and P.T. with help of co-authors; Visualization, H.M.M, C.G.S.,
218 V.K., C.S., S.L.R., O.A., A.S., P.T.; Supervision, H.M.M, C.G.S., C.V., K.H., A.S., O.S.F., P.T.; Project
219 Administration, H.M.M.; Funding Acquisition, H.M.M.

220 Competing interests

221 H.M.M. and V.K. filed a utility model concerning Sylites. C.Sc. is employed at Abbelight.

222 References

- 223 1. Choquet, D., Sainlos, M. & Sibarita, J. B. Advanced imaging and labelling methods to decipher brain cell organization
224 and function. *Nat. Rev. Neurosci.* **22**, 237–255 (2021).
- 225 2. Tyagarajan, S. K. & Fritschy, J.-M. Gephyrin: a master regulator of neuronal function? *Nat. Rev. Neurosci.* **15**, 141–156
226 (2014).
- 227 3. Liu, Y. T. *et al.* Mesophasic organization of GABAA receptors in hippocampal inhibitory synapses. *Nat. Neurosci.* **23**,
228 1589–1596 (2020).
- 229 4. Crosby, K. C. *et al.* Nanoscale Subsynaptic Domains Underlie the Organization of the Inhibitory Synapse. *Cell Rep.* **26**,
230 3284–3297.e3 (2019).
- 231 5. Charrier, C. *et al.* A crosstalk between $\beta 1$ and $\beta 3$ integrins controls glycine receptor and gephyrin trafficking at
232 synapses. *Nat. Neurosci.* **13**, 1388–1395 (2010).
- 233 6. Gross, G. G. *et al.* An E3-ligase-based method for ablating inhibitory synapses. *Nat. Methods* **13**, 673–678 (2016).
- 234 7. Schneider Gasser, E. M. *et al.* Immunofluorescence in brain sections: Simultaneous detection of presynaptic and
235 postsynaptic proteins in identified neurons. *Nat. Protoc.* **1**, 1887–1897 (2006).
- 236 8. Gross, G. G. *et al.* Recombinant Probes for Visualizing Endogenous Synaptic Proteins in Living Neurons. *Neuron* **78**, 971–
237 985 (2013).
- 238 9. Chamma, I. *et al.* Mapping the dynamics and nanoscale organization of synaptic adhesion proteins using monomeric
239 streptavidin. *Nat. Commun.* **7**, (2016).
- 240 10. Maric, H. M. *et al.* Gephyrin-binding peptides visualize postsynaptic sites and modulate neurotransmission. *Nat. Chem.*
241 *Biol.* **13**, 153–160 (2017).
- 242 11. Maric, H.-M., Mukherjee, J., Tretter, V., Moss, S. J. & Schindelin, H. Gephyrin-mediated γ -Aminobutyric Acid Type A and
243 Glycine Receptor Clustering Relies on a Common Binding Site. *J. Biol. Chem.* **286**, 42105–42114 (2011).
- 244 12. Maric, H. M. *et al.* Molecular basis of the alternative recruitment of GABAA versus glycine receptors through gephyrin.
245 *Nat. Commun.* **5**, 5767 (2014).
- 246 13. Fritschy, J. M., Harvey, R. J. & Schwarz, G. Gephyrin: where do we stand, where do we go? *Trends Neurosci.* **31**, 257–
247 264 (2008).
- 248 14. Kuhse, J. *et al.* Phosphorylation of gephyrin in hippocampal neurons by cyclin-dependent kinase CDK5 at Ser-270 is
249 dependent on collybistin. *J. Biol. Chem.* **287**, 30952–30966 (2012).
- 250 15. Specht, C. G. *et al.* Quantitative nanoscopy of inhibitory synapses: Counting gephyrin molecules and receptor binding
251 sites. *Neuron* **79**, 308–321 (2013).
- 252 16. Yang, X., Le Corrion, H., Triller, A. & Specht, C. G. Differential regulation of glycinergic and GABAergic nanocolumns at
253 mixed inhibitory synapses. *EMBO Rep.* **in press**, (2021).
- 254 17. Cappaert, N. L. M., Van Strien, N. M. & Witter, M. P. *The rat nervous system.* (Academic Press, 2015).
255 doi:10.1016/B978-0-12-374245-2.00020-6.
- 256 18. Santuy, A., Rodríguez, J. R., DeFelipe, J. & Merchán-Pérez, A. Study of the size and shape of synapses in the juvenile rat
257 somatosensory cortex with 3D electron microscopy. *eNeuro* **5**, (2018).
- 258 19. Prior, P. *et al.* Primary structure and alternative splice variants of gephyrin, a putative glycine receptor-tubulin linker
259 protein. *Neuron* **8**, 1161–1170 (1992).